JJMIE

Volume 5, Number 5, Oct. 2011
ISSN 1995-6665
Pages 425 - 432

**Jordan Journal of Mechanical and Industrial Engineering**

# Assessment of High Temperatures Sound Transmission Losses and Noise Reduction Factor for a DPF Using a Six-port Acoustic Model

S. M. Fayyad[a], M. N. Hamdan*[,b], S. Abdallah[c]

[a]*Department of Mechatronics, Al-Balqa applied university, Alsalt, Jordan*
[b]*Mechanical Engineering Department, University of Jordan, Amman 11942, Jordan*
[c]*Department of Aerospace Engineering, University of Cincinnati, Cincinnati, OH, 45221, USA*

**Abstract**

We construct a 2-D field model as a modified version of the 1-D model formulated in [1] for the study of sound propagation in a diesel particulate filter (DPF) unit. The modified model is used to evaluate both sound transmission losses and noise reduction factors of a typical DPF unit at high temperatures. The 2-D model is formulated using linearized field Navier-Stocks, energy, and continuity equations but retains the normal as well as transverse component of gas velocity. The temperature, pressure, density, and velocities of gas profiles in the 2-D space and variation with time are assumed to be harmonic. By substituting the differentials of the assumed forms of these variables with respect to both space and time in the governing field equations, a set of three coupled linear 2-D field variation equations for pressure, axial and transverse velocities is obtained. The obtained reduced model is solved analytically using Fourier series approximations for the obtained field variable functions in the reduced model. The approximate solution is used to build a 2-D acoustic model for the exhaust gases emission which accounts for both attenuation and phase shift defining the propagation wave constant. Also the obtained approximate solution is used to determine the acoustics impedance of the DPF unit, soot loading, noise and vibration damping, in addition to calculating the noise reduction factors (NRF). In the present study, unlike previous ones, six, rather than four, roots for wave propagation constant are obtained corresponding to the obtained six port acoustic DPF model. The results obtained using the present six -port model, for selected system parameters are graphically displayed and compared with those available in the open literature using a four- port model. The present model results show, in general, similar qualitative behavior and a significant quantitative improvement of the available results in the open literature obtained using a four port model.



*Keywords:*Acoustic model; Porous media; Darcy law; Wave propagation Constant; Acoustic Transmission Losses

## 1. Introduction

One of the leading technologies for meeting future particulate matter (PM) emission strict standards is the diesel particulate filter (DPF). These devices generally consist of a wall-flow type filter positioned in the exhaust stream of diesel engine vehicles. As the exhaust gases pass through the exhaust system, particulate emissions are collected and stored in the DPF. Because the volume of diesel particulates collected by the system will eventually fill up and even plug the DP filter, a method for controlling trapped particulate matter and regenerating the filter is necessary. The DPF is a superior system in the reduction of particulate matters because it can reduce about 70% of the generated PM. A typical DPF system contains a large number of thin tubes or cavities with a diameter of about (1-2 mm), and (0.15-0.5 cm) length. It is available in several types such as: electric heater, burner (ceramic filter), and fuel additive type; the latter is a honey-comb ceramic. The honey-comb type constitutes an additive supply and an electronic system. In this type Fe is used as an additive whereby iron oxide is formed which reacts with carbon and then it is converted to iron. The DPF is connected at a suitable intervening location along the exhaust gases path through the main exhaust pipe. Thus the noise and vibration characteristics of exhaust system are expected to change and consequently affect the performance of the engine by developing back pressure, changing temperature and velocity of the exhaust gases...etc. Hence building an acoustic model for the DPF is valuable in predicting its effect on the overall performance of the DPF unit.

The acoustic characteristics of the DPF systems have been the subject of many theoretical and experimental investigations, e.g [1-15]. Greevesm et. al [1] studied theoretically the origin of hydrocarbons emission from diesel engines. Their results indicate that a DPF can eliminate some of PM and is a very promising as an after-treatment technique. Yu and Shahed [2] studied the effects of injection timing and exhaust gas recirculation on emissions from a diesel engine. They classified a DPF action as filtration and regenerative processes. Konstandopoulous et al. [3] studied the DPF wall-flow, pressure drop and cooling efficiency. They used Darcy's

* Corresponding author. e-mail: naderhamdan@hotmail.com

law to describe the coupling between neighboring channels of the DPF and to predict system variable changes in the fluctuating fields between the neighboring DFP channels. Peat [4] studied sound propagation in capillary tubes using FEM solutions of simplified wave equations for a visco-thermal fluid flow. Also, Astley and Cumings [5] presented FEM solutions to the axial flow though porous medium, based on simplified wave equation in a visco-thermal fluid. They presented an analysis for the laminar flow with a parabolic velocity distribution and a quadratic flow cross-section. They simplified the governing equations by assuming that the axial gradients to be significantly smaller than the gradients over the cross-section. Employing a simplified analysis presented in [4,6], Dokumaci [7] obtained an exact solution for the case of a plug flow and a circular cross-section. He also presented an acoustic two-port model for a catalytic converter unit, which takes into account the presence of a mean flow , assuming a uniform velocity profile, and the presence of a mean pressure gradient [8]. Ih et al. [9] have developed analytical solutions for sound propagation in capillary cylindrical tubes which assumes a parabolic mean axial flow, and neglects the radial component of the particle velocity. Jeong and Ih [10] presented numerical solutions of the basic governing flow field equations taking into account the radial particle velocity. Their results showed that the radial velocity has a small but noticeable effect on the DPF acoustic behavior. Dokumaci [11] extended his earlier work in [7] to the case of rectangular narrow tubes with a plug flow. His analysis was based on approximate double Fourier sine series expansions for the field variables over the channel cross-section

Allam and Abom [12,13] presented an approximate 1-D, two- ports discrete acoustic model for predicting sound transmission losses for an entire diesel particulate filter (DPF) unit. Their model was based on an approximate treatment of the viscous and thermal losses along the narrow channels of the DPF. Also in this model the steady flow resistance was used to calculate equivalent lumped acoustic impedance. To include the wave propagation effects the monolith was described using coupled wave guide model, where coupling is via the porous walls of monolith. Darcy's law was used to describe the pressure drop in the porous walls. This 1-D wave propagation model yielded a constant, frequency independent, transmission loss and agreed within 1 dB with measured data on a typical hot filter but for low frequencies (<300Hz).

Allam and Abom [14] modified their 1D model in [13] using the classical (exact) Kirchhoff solution for a plane wave propagation in a homogenous , visco-thermal fluid in a rigid narrow tube[15]. The modified model includes a more detailed account for viscous and thermal losses by solving the convective acoustic wave equations for two neighboring channels using Zwikker and Kosten theory. It also uses and modifies the analysis followed by Dokumaci [8] to account for the effect of wall permeability. They used a straightforward linearization and segmentation approach to convert the obtained 1-D model to a 4-th order (4-port) eigenvalue problem whose four eigenvalue are the wave propagation constants. The presented results showed a fair agreement with measured ones for frequencies up to 1000 Hz for a typical filter at operating (hot) conditions. It is noted that the above Allam and Abom [14] model assumes the fields to be constant with respect to space but vary harmonically with time. Fayyad [16], and Hamdan et.al. [17] built, respectively , a four-port and a six-port acoustic models for the DPF following the analysis approach presented in [13, 14] but taking into account the transverse component of gas velocity. They used their models to find transmission losses and noise reduction factor at relatively low temperatures and presented results which showed good agreement with those presented in [14].

In the present work, the analysis developed by Allam and Abom [14] is modified by considering the effect of transverse velocity and is employed to build a 2-D, six -port acoustic model for the entire DPF unit The presented model takes into account field variations both with respect to time and the 2-D space which, to the authors' best knowledge, has been ignored in previous models found in the open literature. The calculated results for the acoustic transmission losses in a typical hot DPF obtained using the present six -port model, for selected system parameters are compared with those presented in [14] using a four-port model.

## 2. Problem Formulation and solution

Following the analyses in [13,14], the DPF is divided into five parts, as shown in Fig. 1. These parts are: the inlet (IN), narrow pipes with impermeable walls (1) and (3), the ceramic section (2), and the outlet section (OUT). The DPF may be manufactured from different materials (Cordierite or Silicon Carbide for example) and in its most common form consists of a substrate of narrow channels. Each channel is approximately square in the cross- section with a width about (1-2) and is blocked at one end. Adjacent channels have this blockage at alternating ends. With this construction exhaust gas may enter at one end, but must pass through the wall of a channel before exiting and is thus termed a wall flow device [13,14]. It is clear from the above description of the DPF construction that the flow in y-direction affects the operation of the DPF, i.e. the transverse velocity can have a significant effect on the flow characteristics and the 1-D flow approximation may not be a realistic one. Therefore, in order to explore this affect the present work considers the flow as 2-D by taking into account the effect of the transverse velocity which was ignored in [,1314].

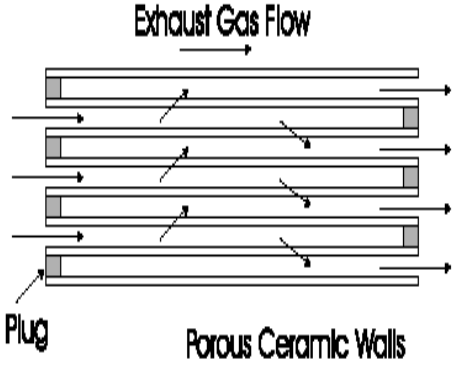


Figure 1: DPF sections and the 2D flow of gases.

## 3. Derivation of the Governing Equations

In deriving the acoustic model for the above described DPF unit the following assumptions, as in [13,14], are made:

- The DPF unit is partially a porous media,
- The transverse "normal" component of velocity , unlike the models in [13,14], will not be neglected: i.e. the flow is treated as a 2-D one.
- The flow is considered as viscous- thermal, incompressible, laminar, steady and a Newtonian ideal gas.
- Chemical reactions are neglected, and pressure, temperature, velocities, and density variations are considered to vary harmonically in both time and the 2-D space.

By considering the field to be 2-D instead of 1-D, the describing field Navier – stocks (momentum), continuity, energy and state equations used in [14], become:

**A.** Navier Stocks equations:

$$\rho_{0j}\left[\frac{\partial u}{\partial t}+u.\nabla U_{0j}\right]=-[\nabla P]_j+\mu[\nabla^2 u_{xj}]_j \tag{1}$$

which, respectively, in x and y directions take the form:

$$\rho_{0j}\left[\frac{\partial u_{xj}}{\partial t}+u_{xj}\frac{\partial U_{0j}}{\partial x}+v_{yj}\frac{\partial U_{0j}}{\partial y}+w_{zj}\frac{\partial U_{0j}}{\partial z}\right]+\rho_{0j}U_{0j}\frac{\partial u_{xj}}{\partial x}= -\frac{\partial P_j}{\partial x}+\mu_j\left(\frac{\partial^2 u_{xj}}{\partial x^2}+\frac{\partial^2 u_{xj}}{\partial y^2}+\frac{\partial^2 u_{xj}}{\partial z^2}\right) \tag{2}$$

$$\rho_{0j}\left[\frac{\partial v_{yj}}{\partial t}+u_{xj}\frac{\partial V_{0j}}{\partial x}+v_{yj}\frac{\partial V_{0j}}{\partial y}+w_{zj}\frac{\partial V_{0j}}{\partial z}\right]+\rho_{0j}V_{0j}\frac{\partial v_{yj}}{\partial y}=-\frac{\partial P_j}{\partial y}+\mu_j\left(\frac{\partial^2 v_{yj}}{\partial x^2}+\frac{\partial^2 v_{yj}}{\partial y^2}+\frac{\partial^2 v_{yj}}{\partial z^2}\right) \tag{3}$$

**B.** Continuity equation**:**

$$\frac{\partial \rho_j}{\partial t}+u_{xj}\frac{\partial \rho_{0j}}{\partial x}+U_{0J}\frac{\partial \rho_j}{\partial x}+\rho_j\frac{\partial U_{0j}}{\partial x}+\rho_{0j}\nabla.u_j=0 \tag{4}$$

**C.** Energy equation

$$\rho_{0j}Cp_j\left[\frac{\partial T_j}{\partial t}+U_{0j}\frac{\partial T_j}{\partial x}+u_{xj}\frac{\partial T_{0j}}{\partial x}\right]+\rho_j Cp_j U_{0j}\frac{\partial T_{0J}}{\partial x}=-\frac{\partial P_j}{\partial t}+U_{0j}\frac{\partial P_j}{\partial x}+\frac{\partial P_{0j}}{\partial x}u_{xj} + K_{thj}\nabla_s^2 T_j \tag{5}$$

**D.** State equation:

With the assumption of ideal gas, the linearized sate equation (linearized ideal gas law) takes the form [14]:

$$\rho_j=\left(\frac{p_j}{R_j T_{0j}}\right)-\left(\frac{\rho_{0j}T_j}{T_{oj}}\right), \tag{6}$$

where

$$\rho_j=\rho_j(x,y,t)$$
$$T_j=T_j(x,y,t) \tag{7}$$
$$P_j=P_j(x,y,t)$$

*x, y* denote, respectively , the longitudinal and transverse channel axes, u, v are the acoustic particle velocities in , respectively, the x and y directions , and j = 1, 2 represent the inlet and outlet pipes, respectively. Also *p, T* and *ρ* are the acoustic pressure, temperature and density, respectively, μ is the shear viscosity coefficient, $k_{th}$ is the thermal conductivity of the fluid, R is the gas constant, *Cp* is the specific heat coefficient at constant pressure, $P_0$, $T_0$ and $\rho_0$ denote the ambient pressure, temperature and density, respectively, $U_0$, $V_0$ denote the axial mean flow velocity and transverse velocity respectively, and $\nabla_s^2$ denotes the Laplacian over the channel cross-section.

To describe the coupling between neighboring channels (which describes the porosity of diesel particulate filter) Darcy's law is applied to the fluctuating fields [14]:

$$p_1-p_2=R_w u_w \tag{8}$$

where a subscript *w* refers to wall, $u_w$ is the acoustic velocity through the wall, $R_w$ is the wall resistance, which is given by $R_w=\mu_w h_t/\sigma_w$, $\mu_w$ is the dynamic viscosity, $h_t$ is the wall thickness, and $\sigma_w$ is the wall permeability.

## 4. Approximate Solution

In order to convert the above nonlinear model into an analytically tractable one, the linearization and segmentation approach presented in [14] is closely followed. Accordingly, and noting that the present model is a 2-D one, the following time and 2-D space harmonic variations for the fields are assumed:

$$u_{xj}=A_0 e^{iwt} \tag{9}$$
$$v_j=B_0 e^{iwt} \tag{10}$$
$$\rho_j=\rho_0 e^{iwt},\quad P_j=P_0 e^{-iwt},\quad T_j=T_0 e^{iwt} \tag{11}$$
$$u_{xj}=-D'(A_0 e^{\Gamma k_1 x}-B_0 e^{-\Gamma k_1 x}) \tag{12}$$
$$v_{yj}=-D'(A_0 e^{\Gamma k_1 y}-B_0 e^{-\Gamma k_1 y}) \tag{13}$$
$$P_{jy}=A_0 e^{\Gamma k_1 y}+B_0 e^{-\Gamma k_1 y} \tag{14}$$
$$P_{jx}=A_0 e^{\Gamma k_1 x}+B_0 e^{-\Gamma k_1 x} \tag{15}$$
$$\rho_{jx}=A_0 e^{\Gamma k_1 x}+B_0 e^{-\Gamma k_1 x} \tag{16}$$
$$\rho_{jy}=A_0 e^{\Gamma k_1 y}+B_0 e^{-\Gamma k_1 y} \tag{17}$$
$$T_{jx}=A_0 e^{\Gamma k_1 x}+B_0 e^{-\Gamma k_1 x} \tag{18}$$
$$T_{jy}=A_0 e^{\Gamma k_1 y}+B_0 e^{-\Gamma k_1 y} \tag{19}$$

Upon substituting equations (9)-(11) into equations (2)-(5), using equation (6) and noting that the assumed equations (12)-(19) are linear, , the governing field equations (2)-(5) take the linear form

$$\rho_{0j}\left[iw+\frac{\partial U_{0j}}{\partial x}\right]u_{xj}+\rho_{0j}\frac{\partial U_{0j}}{\partial y}v_{yj}+(D_{0j}U_{0j}+\frac{\partial}{\partial x})P_{jx}=\mu_j\left(\frac{\partial^2 u_{xj}}{\partial x^2}+\frac{\partial^2 u_{xj}}{\partial y^2}+\frac{\partial^2 u_{xj}}{\partial z^2}\right) \tag{20}$$

$$\rho_{0j}\left[iw+\frac{\partial V_{0j}}{\partial y}\right]v_{yj}+\rho_{0j}\frac{\partial V_{0j}}{\partial x}u_{xj}+(D_{0j}V_{0j}+\frac{\partial}{\partial x})P_{yj}=\mu_j\left(\frac{\partial^2 v_{yj}}{\partial x^2}+\frac{\partial^2 v_{yjj}}{\partial y^2}+\frac{\partial^2 v_{yjj}}{\partial z^2}\right) \tag{21}$$

$$(iw+\frac{\partial U_{0j}}{\partial x})\rho_j+(\frac{\partial \rho_{0j}}{\partial x}+D_{0jj}U_{0j})u_{xj}+\rho_{0j}\nabla.u_j=0 \tag{22}$$

$$(\rho_{0j}Cp_j iw - K_{thj}\nabla_s^2)T_j + \rho_{0j}Cp_j u_{xj}\frac{\partial T_{0j}}{\partial x} + Cp_j U_{0j}\frac{\partial T_{0j}}{\partial x}\rho_{0j} = (iw + U_{0j}\frac{\partial}{\partial x})P_j + (\frac{\partial P_{0j}}{\partial x} - U_{0j}D_{0jj}\rho_{0j})u_{xj} \quad (23)$$

It is noted that by setting to zero in the above equations (e.g by neglecting the transverse velocity) the above model in equations (21)-(24) reduces to the 1-D developed by Allam and Abom [14].

In order to develop an acoustic model for the DPF unit, and to find acoustic impedance, transmission losses, and other needed parameters such as noise reduction factor, equations (21) to (23) must be solved for the variables and These four, homogenous, coupled linear equations with four variables constitute an eigenvalue problem. The condition of a non- trivial solution to these equations leads to a characteristic frequency equation and associated eigenvectors. The eigenvalue problem is obtained as follows, (for more details, see [13,14]. First one assumes

$$\begin{aligned} P_j &= A_j \exp(-i\Gamma k_1 x),\\ u_{xj} &= H_j(x,y,z)P_j,\\ T_j &= F_j(x,y,z)P_j,\\ v_{yj} &= B_j \exp(-i\Gamma k_1 y) \end{aligned} \quad (24)$$

where $A_j, H_j, F_j$ and $B_j$ are constant coefficients. Next substituting the expressions in equation (24) into equations (21)-(23) one obtains

$$\frac{\partial^2 H_j}{\partial x^2} + \frac{\partial^2 H_j}{\partial y^2} + \frac{\partial^2 H_j}{\partial z^2} - i\beta_{xj}^2 H_j = \frac{D_{0j}CM_j}{\mu_j} - \frac{-i\Gamma k_1}{\mu_j} \quad (25)$$

$$\frac{\partial^2 H_j}{\partial x^2} + \frac{\partial^2 H_j}{\partial y^2} + \frac{\partial^2 H_j}{\partial z^2} - i\beta_{jy}^2 H_j = \frac{D_{0j}CM_j}{\mu_j} - \frac{-i\Gamma k_1}{\mu_j} \quad (26)$$

$$\frac{\partial^2 F_j}{\partial x^2} + \frac{\partial^2 F_j}{\partial y^2} + \frac{\partial^2 F_j}{\partial z^2} - \sigma_{jx}^2 F_j = \sigma_{0j}^2 + \sigma_{1j}^2 H_j \quad (27)$$

where

$$\beta_{xj}^2 = (-\Gamma k_1 + \frac{1}{w}\frac{\partial U_{0j}}{\partial x} + \frac{1}{w}\frac{\partial U_{0j}}{\partial y})S_j^2$$

$$\beta_{jy}^2 = (-\Gamma k_1 + \frac{1}{w}\frac{\partial V_{0j}}{\partial x} + \frac{1}{w}\frac{\partial V_{0j}}{\partial y})S_j^2$$

$$\sigma_{jx}^2 = S_j^2 \,\mathrm{Pr}(i - \frac{U_{0j}}{wT_{0j}}\frac{\partial T_{0j}}{\partial x}),$$

$$\sigma_{0jx}^2 = (\frac{\mathrm{Pr}\,S_j^2}{w}\frac{\partial T_{0j}}{\partial x} - \frac{1}{K_{thj}}\frac{\partial P_{0j}}{\partial x} + \frac{S_j^2 M U_{0j}}{wK_{thj}}D),$$

$$\sigma_{jx}^2 = \frac{1}{K_{thj}}(iw - iU_{0j}\Gamma Mw - \frac{Cp_j U_{0j}}{R_j T_{0j}}\frac{\partial T_{0j}}{\partial x}),$$

$$\mathrm{Pr} = \sqrt{\frac{\mu_j Cp_j}{K_{thj}}}$$

Next, following Allam and Abom [14], the following Fourier sine series for the field variables *H* and *F* are assumed:

$$H(x,y,z) = \sum_{m,n} a_{mn} \sin\frac{m\Pi y}{2a_j}\sin\frac{n\Pi z}{2a_j} \quad (28)$$

$$F(x,y,z) = \sum_{m,n} b_{mn} \sin\frac{m\Pi y}{2a_j}\sin\frac{n\Pi z}{2a_j} \quad (29)$$

Then upon substituting equations (28) and (29) into equations (25)-(27), and, as in [1], averaging the mass conservation equation (22), one obtains the following eigenvalue problem:

$$\left[\frac{1}{R_j T_{0j}}(iw + \frac{\partial U_{0j}}{\partial x})(1 - \rho_{0j}R_j < F_j >) + (\frac{\partial \rho_{0j}}{\partial x} + DU_{0j} - 2ik_1\Gamma\rho_{0j}) < H_j >\right]A_j + (-1)^{j-1} * \frac{2\rho_{0j}(A_1 - A_2)}{a_j R_w} = 0 \quad (30)$$

which can be written in matrix form ,using the notation in [14], as follows:

$$\begin{bmatrix} K11 + K21 & -K12 \\ K21 & K12 - K22 \end{bmatrix}\begin{bmatrix} A_1 \\ A_2 \end{bmatrix} = \begin{bmatrix} 0 \\ 0 \end{bmatrix} \quad (31)$$

where

$$K_{1j} = \begin{bmatrix} \frac{R_w a_j}{2\rho_{0j}R_j T_{0j}}(iw + \frac{\partial U_{0j}}{\partial x})(1 - \rho_{0j}R_j < F_j >) + \\ \frac{R_w a_j}{2\rho_{0j}}(\frac{\partial \rho_{0j}}{\partial x} + DU_{0j} - 2ik_1\Gamma\rho_{0j}) < H_j > \end{bmatrix} \quad (32)$$

And

$$K_{2j} = (-1)^{j-1} \quad (33)$$

For a non trivial solution the determinant of the coefficients matrix in equation (31)

$$\begin{vmatrix} K11 + K21 & -K12 \\ K21 & K12 - K22 \end{vmatrix} \quad (34)$$

is set to zero, whereby one obtains the following system characteristic frequency equation:

$$(K11 + K21)(K12 - K22) + K12K21 = 0 \quad (35)$$

The above frequency equation is a 6th order equation for the propagation constant Γ which can only be solved numerically. A specially constructed MATLAB program was used to solve for the six roots of equation (35) for selected values of system parameters. The wave propagation constants, which is dependent on all field parameters, represent two types of waves: one along the positive (forward) and the other is along the negative (backward) directions of the pipe axis and are denoted, respectively ,as usual, by Γ+, and Γ [13,14]. See figures (1) – (4).

Note that the roots (eigenvalues) of equation (35) are complex. The real parts of these wave propagation constants represent the attenuation while the imaginary parts represent the phase shift. The corresponding three complex eigenvectors are given by

$$\begin{pmatrix} \hat{p}_1(x) \\ \hat{p}_2(x) \\ \hat{p}_3(x) \end{pmatrix} = \sum_{n=1}^{6} \hat{a}_n e^{-ik_1\Gamma_n x} e_{j,n} \quad (36)$$

where $\hat{p}(x)$ is the acoustics pressure. , $\hat{a}_n$ is the modal amplitude, $\Gamma_n$ is the calculated wave propagation

constant (eigenvalue) and $e_{j,n}$ , $j=1,2$, are the corresponding components of the 2-D eigenvector, with j=1 corresponds to the inlet and j=2 corresponds to outlet. Note that equation (36) represents the sound field (pressure fluctuation) in filter section. In addition to equation (36) one needs the field volume pressure velocities to calculate the sound transmission losses in the filter. The corresponding volume pressure velocities $\hat{q}_n(x)$ are obtained, as in [14], by dividing equation (36) by the characteristic wave impedance Z, where $Z=\frac{\rho c}{A}$, c= speed of sound, $\rho=$ mass density of the medium, and $A$ is the cross sectional area of the DPF part. This leads to the following expression for the volume pressure velocities $\hat{q}_n(x)$:

$$\begin{pmatrix}\hat{q}_1(x)\\ \hat{q}_2(x)\\ \hat{q}_3(x)\end{pmatrix}=\sum_{n=1}^{6}\hat{a}_n e^{-ik_2\Gamma_n x}e^{'}_{j,n} \qquad (37)$$

where $e^{'}_{j,n}=4a_j^2<H_{j,n}>e_{j,n}$, $k_2=k_1\sqrt{1-8i\beta/k_1}$,

$\beta=C_j\rho_w/dh_jR_w$

$<Hj>=4a_{11}/\Pi^2$. Finally, to calculate the acoustic transmission losses in the DPF unit, one uses equation (36) and (37) to formulate the so called the transformation matrix $T_{DPF}$,

$$[\hat{q}]=[T_{DPF}][\hat{P}] \qquad (38)$$

where the $T_{DPF}$ is a $6\times6$ matrix, which is formed as a product of the individual 2- port transfer matrices corresponding to the five segments of the DPF, and takes the form [14].

$$T_{DPF}=T_{IN}\,T_1\,T_2\,T_3\,T_{out} \qquad (39)$$

The acoustic transmission losses *TL* are then calculated using the relation [14]

$$TL=20\log|T_{DPF}/2| \qquad (40)$$

In addition, the noise reduction factor *NRF* can be calculated by using the following equation:

$$NRF=LP_2-LP_1=20\log\frac{P_2}{P_1} \qquad (41)$$

## 5. Results and Discussion

The wave propagation constant $\Gamma_n$, transmission losses TL and the noise reduction factor NRF were calculated, for selected system parameters, using equations (35), (40) and (41). A MATLAB program was used to carry out all needed calculations. The results obtained were for the cases: hot at $500^0C$ and at 1000 C . For the two cases the frequency was varied over the range $400-1000$ Hz. Also results were obtained for two cases: one with soot layer and the other with no soot layer. Samples of the obtained for different types of DPF are displayed in figurers (2) – (14).
From these figures the following points are made:

- Both transmission loses and noise reduction factor for the typical filter and other types of DPFs tend to increase as frequency increases.
- Figures (2)-(5) show that the wave propagation through the DPF unit suffers both attenuation and phasing shift, and both attenuation and phase shift decrease as the shear wave number increases.
- Transmission losses for the case of soot layer formation are significantly higher than those with no soot layer formation.
- The present six-port model show similar tends concerning transmission losses as those presented in [14] using a four-port model. However the present six-port model result, which takes into account the effect of the field transverse velocity , are in closer agreement with the experimental ones presented in [14] than the analytical four-port model results presented obtained in [14] which ignore this effect. Therefore one may conclude that ignoring the transverse velocity can have a significant effect on the evaluation of acoustic transmission losses for a DPF unit.

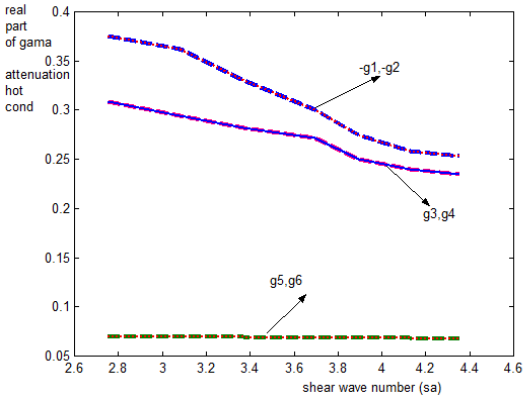


Figure 2: Real part of wave propagation constant Γ, denoted here as g, vs. shear wave number (phase shift), Γ1 and Γ2 propagation constants for uncoupled waves, Γ3 and Γ4 propagation constants for coupled waves, Γ5 and Γ6 represent the interfering parts, time and 2-D space harmonic variation, and under hot conditions(T=500 ˚C ).

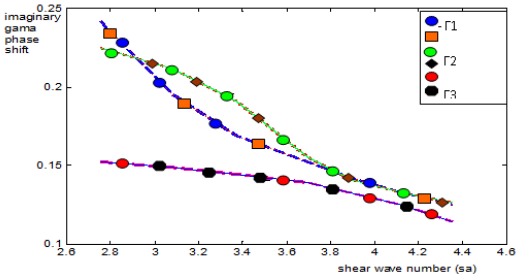


Figure 3: Imaginary part of Γ vs. shear wave number (phase shift), Γ1 and Γ2 propagation constants for uncoupled waves, Γ3 and Γ4 propagation constants for coupled waves, Γ5 and Γ6 represent the interfering parts, under hot conditions (T=500 ˚C).

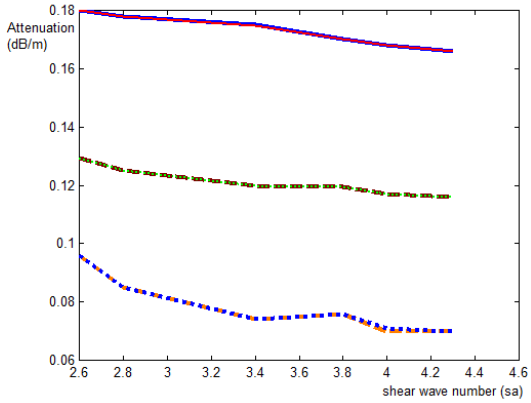


Figure 4: Real part of Γ vs. shear wave number, ….Γ1, and--- Γ2 are propagation constants represent uncoupled waves, ….Γ3, and ----Γ4 propagation constants for coupled waves, ….Γ5, and -----Γ6 under hot conditions (T=1000˚C).

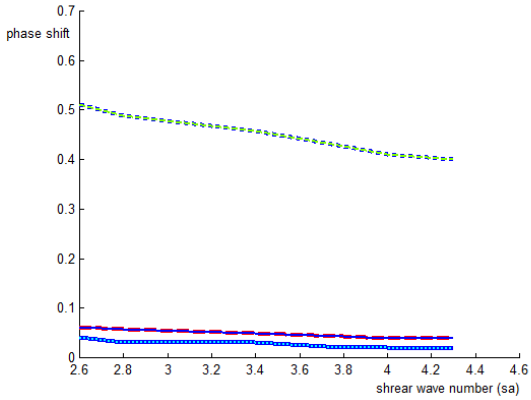


Figure 5. Imaginary part of Γ against shear wave number, ----Γ1, and--- Γ2 are propagation constants represent uncoupled waves, ….Γ3, and ----Γ4 propagation constants for coupled waves, ….Γ5, and …..Γ6, under hot conditions (T=1000˚C).

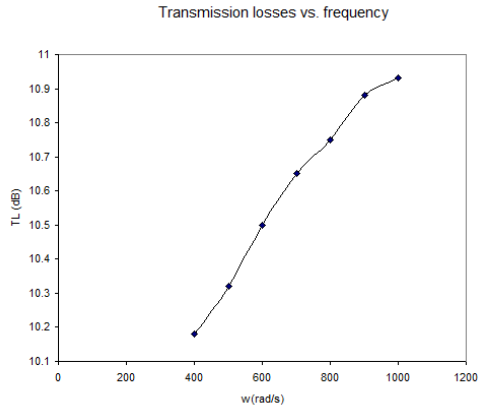


Figure 6: transmission losses vs. frequency in the case of hot conditions (T=500 C) for typical filter for the case of no soot layer, Mach=0.02 and space and time variation case.

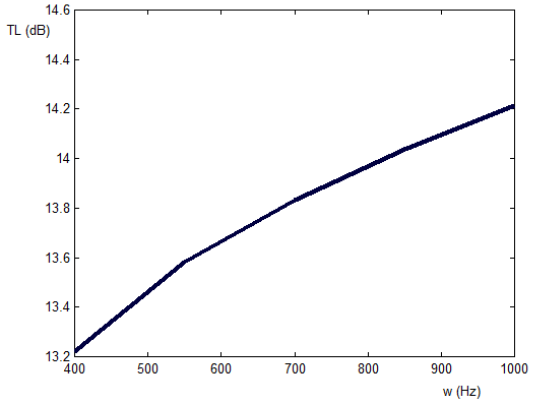


Figure 7: Transmission losses vs. frequency in the case of hot conditions (T=500C) for typical filter for the case of with soot layer, Mach=0.02, and Plane and time variation case.

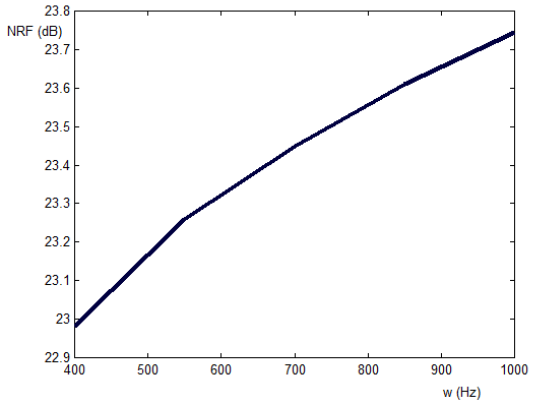


Figure 8: NRF vs. frequency for typical DPF in the case of hot conditions, (With no soot layer). Mach=0.02, in the case of plane and time variation.

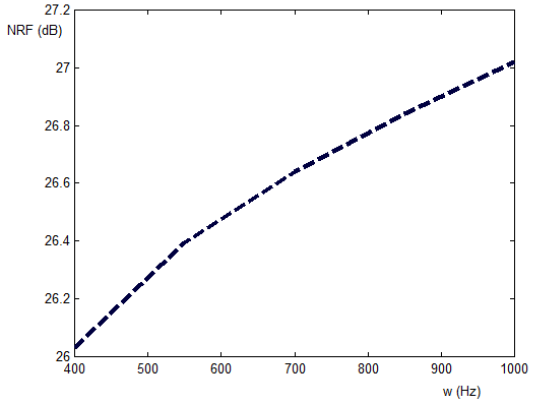


Figure 9: NRF vs. frequency for typical DPF in the case of hot conditions, (With soot layer). Mach=0.02, in the case of plane and time variation.

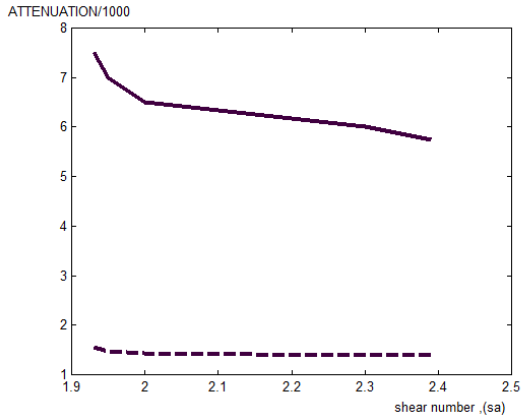


Figure (10): Attenuation against shear number comparison: present study, results in [14] . Hot conditions.

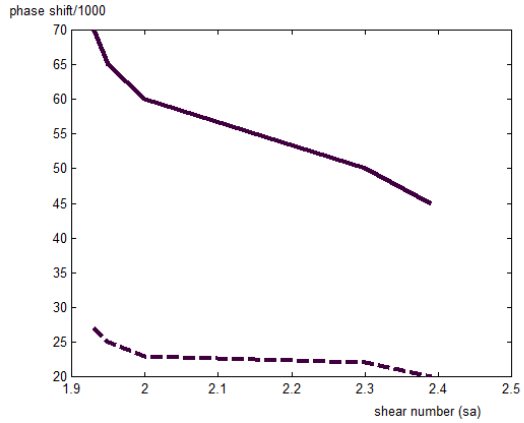


Figure (11): Phase shift against shear number comparison: present study, results in [14]. Hot conditions .

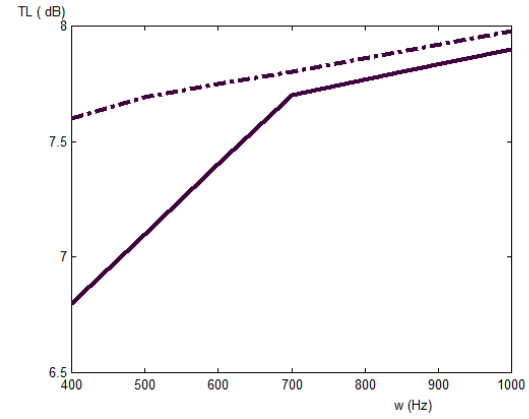


Figure (12): transmission losses against frequency for RC: 200/12 DPF unit type under the case of hot conditions compared with experimental results in [14], present study, Experimental results [14]; (with no soot layer), and Mach=0.02.

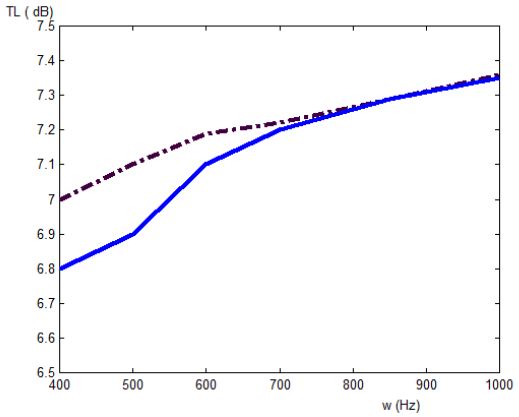


Figure (13): transmission losses against frequency for EX: 100/17 DPF unit type under the case of hot conditions compared with experimental results in [14]. Present study, experimental results [14]; (with no soot layer), and Mach number=0.02.

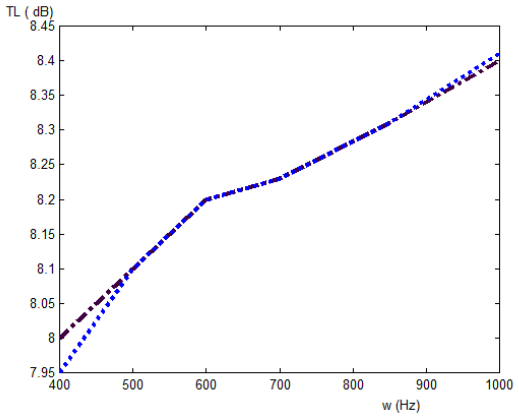


Figure 14: Transmission losses against frequency for EX80: 200/14 DPF unit type under the case of hot conditions compared with experimental results in [14]. Present study, experimental results [14]; with no soot layer and March number =.02.

## 6. Conclusion

An approximate analytical 2-D, six-port acoustic model for a DPF unit is presented. The development of this approximate model follows closely the 1-D, four-ports analysis by Allam and Abom by taking into account the effect of transverse velocity. The results of the present study show similar qualitative behavior and a significant quantitative agreement improvement of the available experimental results for a clean ( no soot formation) in the open literature than a four -port model and at room temperature only . Further validation of this model is required by comparing its predictions to those obtained using numerical analysis of the full governing nonlinear field equations and to results of tests on filter connected to running real engines to ensure hot conditions and soot layer formation.

## 7. References


[1] G. Greevesm, I. M. Khan, C. H. T. Wang, I. Fenne, "Origins of hydrocarbon emission from diesel engines". Society of Automotive Engineering, SAE Paper No. 770259, 1977, 02-01.

[2] R. Yu, Yu, S. M. Shahed, "Effects of injection timing and exhaust gas recirculation on emissions from a DI diesel engine". Society of Automotive Engineering, SAE Paper No. 811234, 1981.

[3] A. G. Konstandopoulos, J. H. Johnson, "Wall-flow diesel particulate filters - their pressure drop and collection efficiency", Society of Automotive Engineering, SAE Paper No. 890405, 1989.

[4] K. S. Peat, "A first approximation to the effects of mean flow on sound propagation in capillary tubes", Journal of Sound and Vibration Vol. 175, 1994, 475–489.

[5] R. J. Astley, A. Cummings, A., "Wave propagation in catalytic converter formulation of the problem and finite element scheme". Journal of Sound and vibration, Vol.188 , No. 5, 1995, 635–657.

[6] P. Davies, "Practical flow duct acoustics". Journal of Sound and Vibration, Vol. 124 , 1988, 91–115.

[7] Dokumaci, "An approximate dispersion equation for sound waves in a narrow pipe with ambient gradients". Journal of Sound and Vibration, Vol. 240, No. 4, 2001, 637–646.

[8] Dokumaci, "Sound transmission in narrow pipes with superimposed uniform mean flow and acoustic modeling of automobile catalytic converters", Journal of Sound and Vibration, Vol. 182 , 799–808, 1995.

[9] J.-G Ih, C. M. Park, H-J. Kim , " A model for sound propagation in capillary ducts with mean flow". Journal of Sound and Vibration Vol. 190, No.2, 163–175, 1996.

[10] K.-W. Joeng, J.-G. Ih, (1996). "A numerical study on the propagation of sound through capillary tubes with mean flow", Journal of Sound and Vibration, Vol. 198, No. 1, 67–79, 1996.

[11] E. Dokumaci, "On transmission of sound in circular and rectangular narrow pipes with superimposed mean flow". Journal of sound and vibration, Vol. 210, No. 3, 1998, 375–389,1998.

[12] S. Allam, M. Abom, "On Acoustic modeling and testing of diesel particulate filters." Proceedings of Inter. Noise Conference, Paper No. 250, 2002 .

[13] S. Allam, S. M. Abom, "Acoustic modeling and testing of diesel particulate filters ."Journal of Sound and Vibration, Vol. 288 (1/2) , 255–273, 2005.

[14] S. Allam, S. M. Abom, "Sound propagation in an array of narrow porous channels with application to diesel particulate filters". Journal of Sound and Vibration, Vol. 291, 882-901, 2006.

[15] D. H. Keefe, " Acoustical wave propagation in cylindrical ducts: transmission line parameter approximations for isothermal and non-isothermal boundary conditions." Journal of the Acoustical Society of America, Vol.75, No. 1, 58–62, 1984.

[16] S. Fayyad, "Sound propagation in porous media with application to diesel" particulate filters." PhD Thesis, University of Jordan, 2006.

[17] M. N. Hamdan, S. Fayyad, S., M. A. Hamdan, "Six-port model for sound propagation in a porous media with applications to diesel particulate filters", AMME-13 Conference , Cairo-Egypt- Paper No. 62, 2008.